Akademie věd České republiky
Ústav teorie informace a automatizace

Academy of Sciences of the Czech Republic
Institute of Information Theory and Automation

RESEARCH REPORT

M. Zima, P. Tichavský, V. Krajča:

Automatic Removal of Sparse Artifacts in Electroencephalogram

No. 2289 November 2010

ÚTIA AV ČR, P. O. Box 18, 182 08 Prague, Czech Republic
E-mail: utia@utia.cas.cz

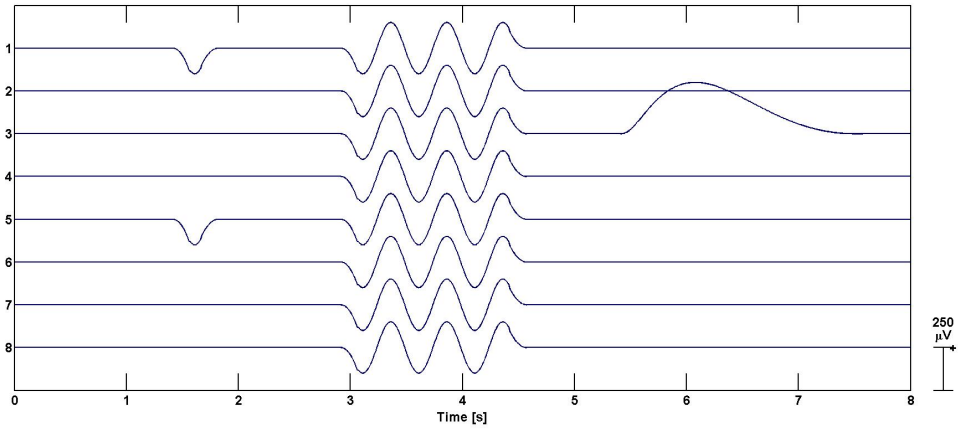

Figure 1: Models of artifacts. The first one represents an eye blinking, the second a movement artifact and the third an unstuck electrode.

1 Introduction

The EEG describes the electric activity of the brain and contains important information about the state of the patient's health. Visual analysis of the EEG record is a difficult and tedious task. An automatic quantitative methods of objective analysis are needed.

The EEG signal is almost always contaminated by various kinds of parasitic signal (artifacts), i.e. electrical biosignals detected along the scalp by an EEG machine, but originating from non-cerebral sources. They may be caused by muscle activity (EMG artifact), movement of the body, eye-induced artifacts (eye blinks and movements) etc. The amplitude of the artifacts can be quite large relative to the size of the amplitude of the cortical signals of interest. This is one of the reasons why it needs an expert to correctly interpret EEGs clinically and why the artifact presence can damage the results of automatic detection and identification of significant EEG graphoelements. Possible models of the considered artifacts are in figure 1.

This report extends the algorithm for removing artifacts from EEG signal, which was proposed in [15]. The extension is based on using wICA technique presented by Castellanos and Makarov in [3].

The report consists of six sections. The first section aims on independent component analysis method (ICA) for separation of artifacts from short-term[1]

[1]The short-term means ≈2000 samples, what is ≈16s with 128Hz sampling or ≈8s with 256Hz

signal. The second section presents the wICA approach introduced in [3]. An overview about discrete wavelet transformation (DWT) and its application in wavelet denoising are included. The usage of ICA on signals with a lower rank is discussed in the third section. In the fourth section an *ad hoc* criterion for automatic detection of artifacts is proposed. The fifth section presents a robust method for processing of a long-term signal. The last section shows some examples on both semi-simulated and real EEG signals.

2 Independent component analysis

Methods of the Independent Component Analysis (ICA) have been shown very useful in analyzing biomedical signals, such as EEG and MEG [10, 14, 8, 7]. In particular, it appears that these methods have an ability to separate artifacts which exceeds in magnitude from useful biological signals.

The aim of the ICA is to convert multichannel signal X via invertible linear transformation to so called independent components S. Actually, the separated components may not be truly statistically independent, but they are independent as much as possible according to some criterion. In biomedical signal processing they proved capable to separate responses of different origin, e.g. electrocardiogram (ECG) of a pregnant woman from ECG of her baby, or an unwanted interference from a relevant signal [9].

Symbolically, the considered model is,

$$X = AS \tag{1}$$

where S represents a $d \times N$ matrix, composed of d rows, so that each row denotes one independent component.

The goal of the ICA is to estimate the mixing matrix A or, equivalently, the de-mixing matrix $W = A^{-1}$ or, equivalently, the original source signals S. Without any loss of generality we can assume that the independent components are centered (have sample mean equal to zero) and scale normalized so that their sample mean square is equal to 1.

In the context of the artifact removal it is desirable to have unwanted signals concentrated in a few separated components. The original signal can be reconstructed without the artifact components (i.e. the components containing artifacts) using the estimated matrix A.

In the EEG signal processing, the most widely studied ICA algorithms are Infomax, [10], SOBI, [1], and FastICA, [6]. While SOBI is based on the second-order statistics, the other two algorithms use high-order statistics. SOBI was advocated in [12]. In this paper, we use an algorithm BGSEP (Block Gaussian Separation), [11] implemented through [13]. BGSEP is based on second-order

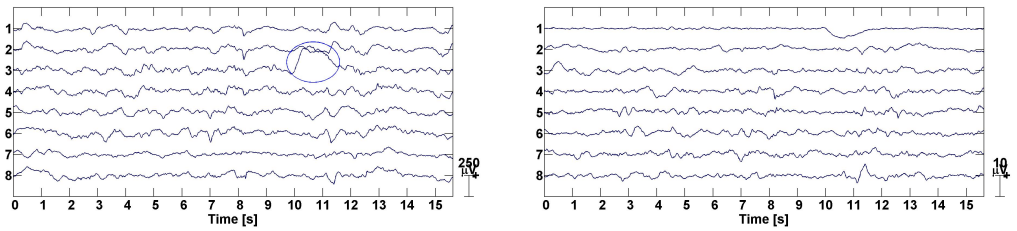

Figure 2: Short EEG with artificially added artifact (marked by circle) and separated components provided by BGSEP. The artifact has been separated into the first component.

statistics as SOBI is, but it uses the nonstationarity of separated signals. While SOBI is done by approximate joint diagonalization (AJD) of a set of time-lagged covariance matrices of the signal (the mixture), BGSEP performs an AJD of zero lag covariance matrices in a partition of the signal. The output of BGSEP is A^{-1}.

An illustrative example of ICA application is in figure 2.

3 Application of ICA on low rank signal

If channels are linearly dependent (i.e the signal has lower rank than the number of channels), there is a requirement for retaining this dependency. However when ICA is applied and one of the components is omitted due to the presence of an artifact, generally the reconstructed signal will not satisfy the original linear dependency, and even the ICA itself might be problematic due to low conditional number of the data.

To overcome this, only linearly independent part of original signal should be processed. Toward this goal, the original signal S is transformed via suitable linear transformation M into a full rank signal S_{sub} of a lower dimension. Then, the algorithm for removing artifacts is applied, and original processed signal $\hat{S}$ is obtained from $\hat{S}_{sub}$ via inverse transformation M_{inv}. Written schematically

- compute $S_{sub} = MS$,
- process S_{sub} and get $\hat{S}_{sub}$,
- compute $\hat{S} = M_{inv}\hat{S}_{sub}$.

Note that the processed signal $\hat{S}$ will satisfy the same dependency as original signal S.

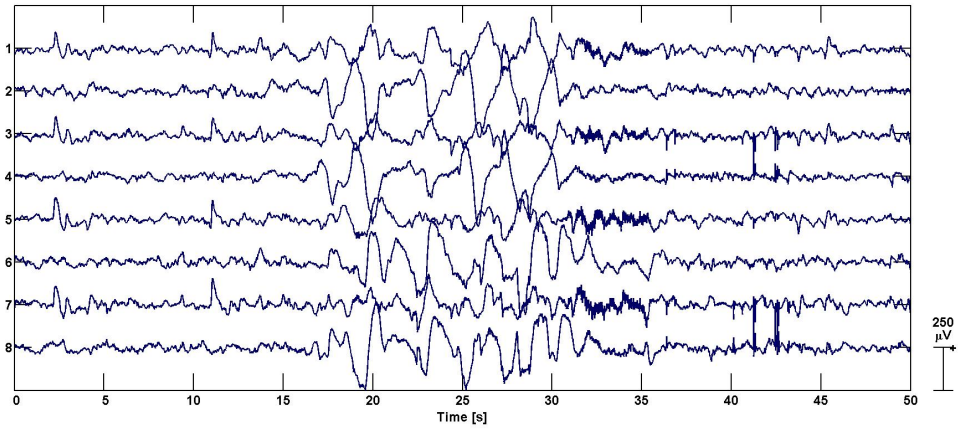

Figure 3: Bipolar EEG record. The channels 1-8 stand for FP1-C3, C3-O1, FP1-T3, T3-O1, FP2-C4, C4-O2, FP2-T4, and T4-O2, respectively.

An example of low rank signal can be EEG record obtained by bipolar montage, shown in figure 3. In bipolar EEG each channel represents the difference between two adjacent electrodes.

Due to bipolar montage, the channels s_i satisfy equations

$$s_1 = -s_2 + s_3 + s_4 \tag{2}$$

$$s_8 = s_5 + s_6 - s_7. \tag{3}$$

Then the original processed signal $\hat{S}$ can be obtained from the processed sub-signal $\hat{S}_{sub}$ by computing s_1 and s_8 according to equations (2) and (3). Thus, the transformation via M_{inv} has the form

$$\hat{S} = \begin{pmatrix} -1 & 1 & 1 & 0 & 0 & 0 \\ 1 & 0 & 0 & 0 & 0 & 0 \\ 0 & 1 & 0 & 0 & 0 & 0 \\ 0 & 0 & 1 & 0 & 0 & 0 \\ 0 & 0 & 0 & 1 & 0 & 0 \\ 0 & 0 & 0 & 0 & 1 & 0 \\ 0 & 0 & 0 & 0 & 0 & 1 \\ 0 & 0 & 0 & 1 & 1 & -1 \end{pmatrix} \hat{S}_{sub} \tag{4}$$

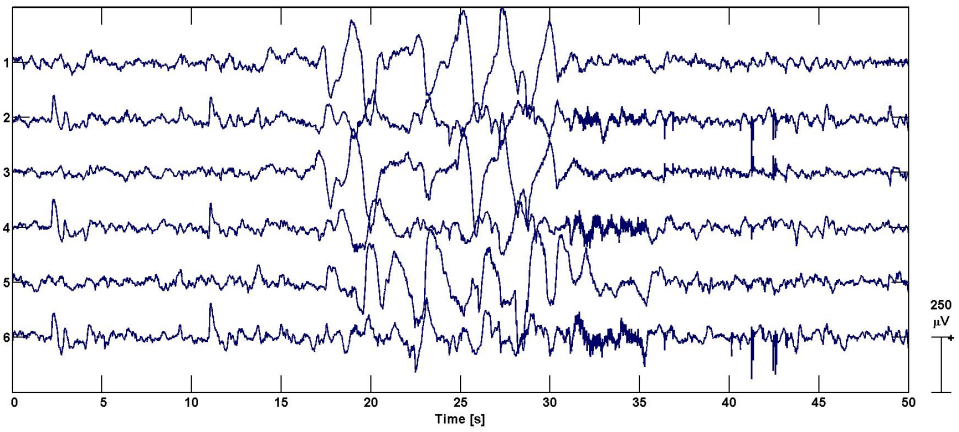

Figure 4: The full rank subsignal S_{sub} of signal from figure 3.

Transformation matrix M can be computed as a pseudoinverse of M_{inv},

$$M = (M_{inv}^T M_{inv})^{-1} M_{inv}^T = \frac{1}{4} \begin{pmatrix} -1 & 3 & 1 & 1 & 0 & 0 & 0 & 0 \\ 1 & 1 & 3 & -1 & 0 & 0 & 0 & 0 \\ 1 & 1 & -1 & 3 & 0 & 0 & 0 & 0 \\ 0 & 0 & 0 & 0 & 3 & -1 & 1 & 1 \\ 0 & 0 & 0 & 0 & -1 & 3 & 1 & 1 \\ 0 & 0 & 0 & 0 & 1 & 1 & 3 & -1 \end{pmatrix} \tag{5}$$

The full rank subsignal of signal from figure 3 is in figure 4.

4 Wavelet enhanced ICA

When dealing with real EEGs, ICA estimated independent components captured beside of present artifacts, frequently contain a considerable amount of cerebral activity. Rejection of such components causes a loss of a part of the cerebral activity and, consequently, distortion of the artifact free EEG. Figure 5 and 6 illustrates that.

To overcome this situation, we use method of wavelet enhanced ICA (wICA) proposed by Castellanos and Makarov in [3]. This method is based on discrete wavelet transform and its application is called the wavelet denoising.

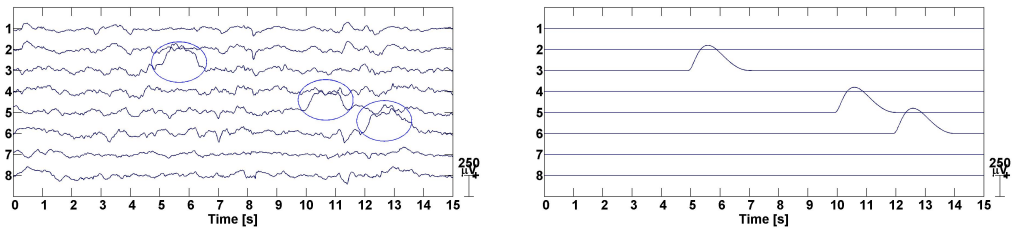

Figure 5: Original signal with artificially added artifacts (marked by circles). The right part of the figure shows the added artifacts.

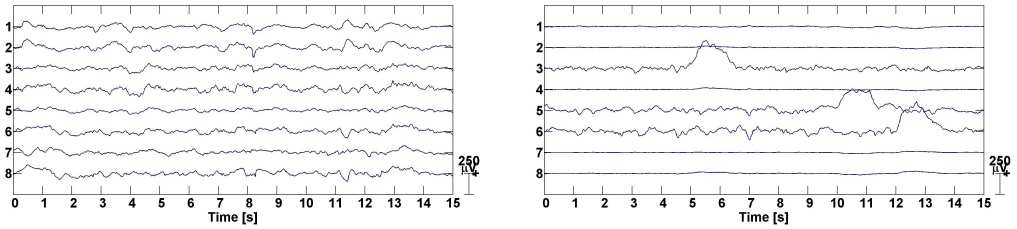

Figure 6: The signal from the figure 5 processed by BGSEP. The right part of the figure shows the estimated artifacts.

4.1 Discrete wavelet transform

A signal S can often be better processed if is written as a linear decomposition

$$S(t) = \sum_l a_l \psi_l(t), \tag{6}$$

where l is an integer index for finite or infinite sum, a_l are real-valued expansion coefficients, and $\{\psi_l(t)\}$ is a set of real-valued functions of t called the expansion set. If the expansion set is an orthogonal basis, then the expansion coefficients can be calculated as

$$a_l = \langle S, \psi_l \rangle = \int S(t)\psi(t)\mathrm{d}t. \tag{7}$$

For example in the discrete Fourier transform (DFT), the ψ_l are goniometric functions with different frequencies. Therefore, the DFT can be well used for localizing the signal frequencies. However is unsuitable to describe a discontinuities or a sharp corners because it takes a large number of Fourier components.

For the wavelet expansion, a two-parameter system is used. Therefore

$$S(t) = \sum_k \sum_j a_{j,k} \psi_{j,k}(t), \tag{8}$$

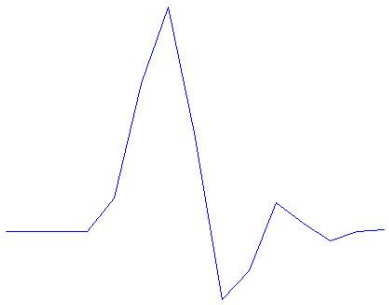

Figure 7: Wavelet ψ_{D6}. This wavelet was developed by Daubechies in [4].

where both j and k are integer indices and the $\psi_{j,k}(t)$ are the wavelet expansion functions that form an orthogonal basis.

Mostly used case is when the $\psi_{j,k}$ are generated from a single wavelet (called mother wavelet) with compact support by simple scaling and translation

$$\psi_{j,k}(t) = 2^{j/2}\psi(2^j t - k) \qquad j,k \in \mathbb{Z}. \tag{9}$$

Because of this, the wavelets are well suited in localizing the signal both in frequency and time domains. An example of possible choice of the mother wavelet is shown in figure 7.

The set of $a_{j,k}$ is called the discrete wavelet transform (DWT). The expansion coefficients can be computed very efficiently by so-called *filter bank*. The filter bank is a structure that decomposes a signal into a collection of subsignals. In DWT, these subsignals are the wavelet coefficients at different time domains. The decomposition into filter bank is done recursively. For more about filter bank and wavelets, see [2].

4.2 Wavelet denoising

Wavelet denoising (WD) is based on taking the discrete wavelet transform (DWT) of a signal. The transformed signal is passed through a filter, which removes coefficients below a certain threshold and then, the inverse DWT is taken. The basic idea of WD of signal S can be written in following scheme

- compute the DWT of S, i.e. compute the wavelet coefficients $a_{j,k}$
- for all $a_{j,k}$ perform the so-called hard thresholding

$$\hat{a}_{j,k} = \begin{cases} a_{j,k} & \text{if} |a_{j,k}| \geq t, \\ 0 & \text{if } |a_{j,k}| < t. \end{cases}$$

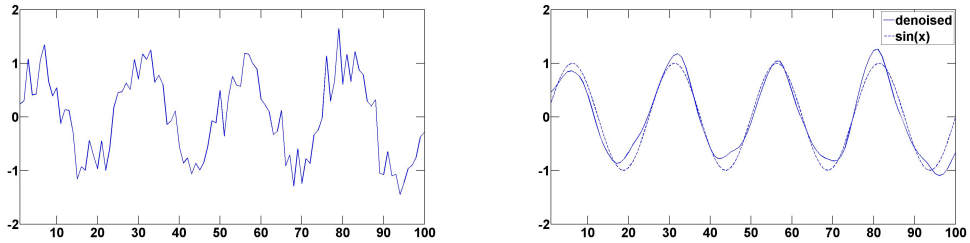

Figure 8: The original signal, which is to be denoised, has the form $x(t) = \sin(t) + 0.3e(t)$, where $e(t) \sim N(0,1)$. The signal after WD is in the right part. For comparison, the signal $\tilde{x}(t) = \sin(t)$ is also shown.

or the so-called soft thresholding

$$\hat{a}_{j,k} = \begin{cases} \operatorname{sgn}(a_{j,k})(|a_{j,k}| - t) & \text{if } |a_{j,k}| \geq t, \\ 0 & \text{if } |a_{j,k}| < t. \end{cases}$$

- compute the inverse DWT $\hat{S}$ using wavelet coefficients $\hat{a}_{j,k}$.

This scheme was proposed by Donoho in [5].

If a signal has its energy concentrated in a small number of wavelet dimensions, its coefficients will be large relatively to any other signal or noise that has its energy spread over a large number of coefficients. Therefore, WD is able to remove noise and minor parts of the signal because of the concentrating ability of the wavelet transform. An illustrative example of WD is in figure 8.

For more information about the WD technique, see [2].

4.3 Wavelet enhanced ICA

In order to use WD for artifact removing, the partly separated component s is assumed to be composed of high amplitude artifact $a(t)$ and a low amplitude residual neural signal $n(t)$. Thus

$$s(t) = a(t) + n(t). \tag{10}$$

Using properties of the signals $a(t)$ and $n(t)$ we can estimate them. Asume, that the artifact $a(t)$ has high magnitude (power) and is localized in the time and/or in frequency domains, while $n(t)$ is of low amplitude and has abroad band spectrum. These properties are in accordance with conditions of WD usage where artifact $a(t)$ is the major part of the signal and $n(t)$ as a noise. For removing artifact without loss of residual neural signal $n(t)$ an estimate of $a(t)$ proposed by WD is subtracted from $s(t)$. This is used in the inverse ICA transform. Schematically, removing artifacts from signal X using wICA can be described as follows

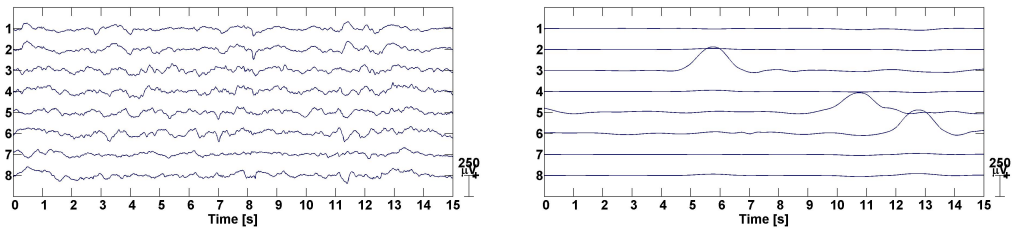

Figure 9: Signal from figure 5 processed by algorithm based on ICA. Right part of the figure shows the estimated artifacts.

- compute the ICA $S = WX$, $S = (s_1, \ldots, s_d)$
- for $i = 1 : d$

  if s_i contains an artifact

  using WD compute $\hat{a}_i(t)$ from $s_i(t)$

  remove the artefact from component, thus $\hat{s}_i(t) := s_i(t) - \hat{a}_i(t)$

  else

  $\hat{s}_i(t) := s_i(t)$
- reconstruct original signal without artifacts via inverse ICA $\hat{X} = W^{-1}\hat{S}$

In our implementation the realization of WD is performed by MATLAB function $\hat{a}_i(t)$=`wden(`$s_i(t)$`,'sqtwolog','s','one',7,'db6')`, where the parameters stand for

- 'sqtwolog' – the threshold selection rule, 'sqtwolog' stands for universal threshold $\sqrt{(2log(.))}$,
- 's' – the type of thresholding, 's' is for soft thresholding,
- 'one' – multiplicative threshold rescaling, 'one' means that the signal will not be rescaled (due to ICA implementation, the variance of $s_i(t)$ is equal to 1),
- 7 – wavelet decomposition will be performed at level 7,
- 'db6' – the desired orthogonal wavelet will be ψ_{D6}, see figure 7.

Advantages of wavelet improvement can be seen in figure 9. There is a result of processing the signal from figure 5 by wICA.

5 Automatic detection of artifact component

If an automatic algorithm for removing artifacts is to be proposed, an criterion for artifact component is needed. This section presents a simple ad hoc criterion which is suitable in our application.

All considered artifacts have one feature in common: their duration is short compared to the chosen frame length. Such signal components will be called *sparse* in the time domain. Sparse components have large maximum absolute value (due to the presence of the artifact), and simultaneously the median of the absolute value close to zero (due to $\mathrm{std}[s_i^{(j)}] = 1$, where "std" stands for a standard deviation). We propose following definition of sparsity

$$\mathrm{sparsity}(s^{(j)}) = \frac{\max[|s_i^{(j)}|]}{\mathrm{std}[s_i^{(j)}]} \log\left(\frac{\mathrm{std}[s_i^{(j)}]}{\mathrm{median}[|s_i^{(j)}|]}\right), \tag{11}$$

where $s^{(j)} = (s_1^{(j)}, \ldots, s_N^{(j)})$ is the $j-$th i is the time index, and N is the number of samples in the frame.

We note, however, that the choice of the criterion of the sparsity is not crucial for our method, and our criterion can be easily replaced by another user-chosen criterion and corresponding sparsity threshold.

For any definition of the sparsity, the component is regarded to be sparse (artifact), if its sparsity exceeds some threshold. The threshold is a variable of the proposed artifact removal procedure. A higher value of the limit means a more conservative (a weaker) artifact reduction. Note that the usage of WD leads to a stronger robustness against removing cerebral activity in the cases where too low threshold is used.

6 Processing of long-term signal

Real EEG records are usually long. If the artifact removal is performed simply frame by frame, the performance may not always be satisfactory. Some artifacts can fall into two adjacent frames and are masked. In addition, there is always a nonzero probability of artifact presence in a reconstruction, and a probability of removing some useful signal part. For these reasons, we found it useful to perform the artifact removal in multiple frames three times, each time with a different partitioning of the signal into frames. Each partitioning gives one possible artifact-free reconstruction of the whole signal. These reconstructions are combined together in a special way so that the final reconstruction is generally smoother and more artifact-free than the partial reconstructions.

Let N denotes the length of one frame. For simplicity we assume that the length of the signal is $L = nN$, for suitable integer n. At first, the signal is

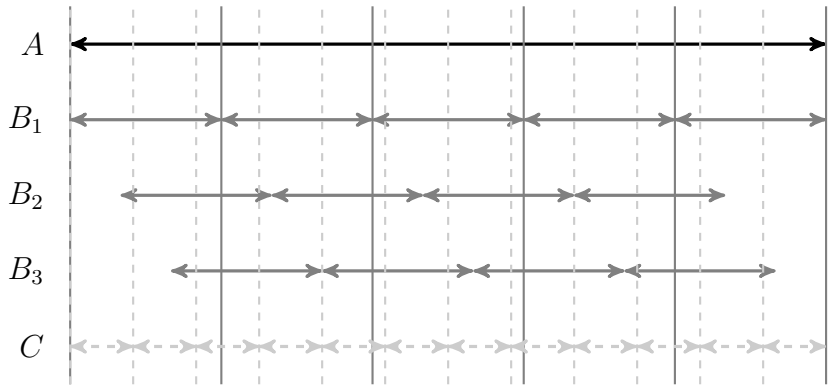

Figure 10: In three independent steps the signal A is divided into frames B_i where ICA (or wICA) is applied. After obtaining partial reconsturctions, they are combined channel by channel, segment by segment into final reconstruction. Location of frames C is schematicaly shown.

divided into frames $[1 + (k-1)N, kN]$ where $k = 1 \dots n$. In these frames the algorithm for removing artifacts is applied. The second partial reconstruction is done in similar way with frames $[1 + N/3 + kN, N/3 + (k+1)N]$ for $k = 1 \dots n-1$. The third partitioning is $[1+2N/3+(k-1)N, 2N/3+kN]$ with $k = 1 \dots n-1$. For the second and the third reconstruction no ICA is performed at the beginning and at the end of the signal. In this case only first reconstruction is used in order to get final reconstruction.

Combination of three reconstructions into one proceeds sequentially, independently channel by channel, in segments of length T which are generally shorter than the frames where ICA has been applied. Again for simplicity let $L = mT$, where m is suitable integer. Hence segments have the form $[1 + (k-1)T, kT]$ for $k = 1 \dots m$.

Division of the signal into frames and segments is shown schematically in figure 10.

The method for combination partial reconstructions into one follows. Let r_1, r_2 and r_3 denote three partial reconstructions in k-th channel in the l-th segment. Let μ_i denote maximum absolute value of elements of r_i. We assume that at least one partial reconstruction is artifact free. Without any loss of generality we assume that $\mu_1 \leq \mu_2 \leq \mu_3$. Therefore, at least r_1 is artifact free. Let $\rho_{ij} = \|r_i - r_j\|^2$ denote squared Euclidean distances of the reconstructions and let ρ_r denote the average squared norm $\|r\|^2$ of a segment r of the same length as r_i, randomly or systematically chosen in the whole available signal.

The final reconstruction r is obtained as the average of one, two, or all three partial reconstructions according to validity of condition (12) and (13),

see diagram 11.

$$\max(\rho_{12}, \rho_{13}, \rho_{23}) \leq 2 \min(\rho_{12}, \rho_{13}, \rho_{23}) \tag{12}$$

$$\max(\rho_{12}, \rho_{13}, \rho_{23}) > 2\rho_r. \tag{13}$$

Performance of combination procedure is shown in illustrative example in figure 12. The figure shows three possible reconstructions which still contain some artifacts (artifacts has been added artificially). One of the reconstructions also simulates the situation when all signal has been removed due to an ICA or automatic artifact detection failure. The fourth channel contains the final reconstruction.

7 Examples of artifacts removal

7.1 Artificial artifacts

In this part we present an example of performance of the proposed algorithm on EEG signal with artificially added artifacts (models are in figure 1).

Original signal and added artifacts are in figure 13. The signal was sampled by 128Hz and is unipolar.

The figure 14 shows the processed data. The frames for wICA had 2000 samples (≈15s), and the fragments for the reconstruction had 128 samples (=1s). Limit sparsity was 2.

7.2 Real artifacts

In this part we present an example of performance of the proposed algorithm on EEG signal with real artifacts.

Original signal and added artifacts are in figure 15. The signal was sampled by 128Hz and is bipolar.

The figure 16 shows the processed data . Settings of the algorithm were the same as before with artificial artifacts.

Advantages of usage wICA can be seen by comparison of figure 16 and figure 17, which shows the signal processed with ICA without wavelet enhancement.

Performance of combination procedure in this case is shown in figure 18.

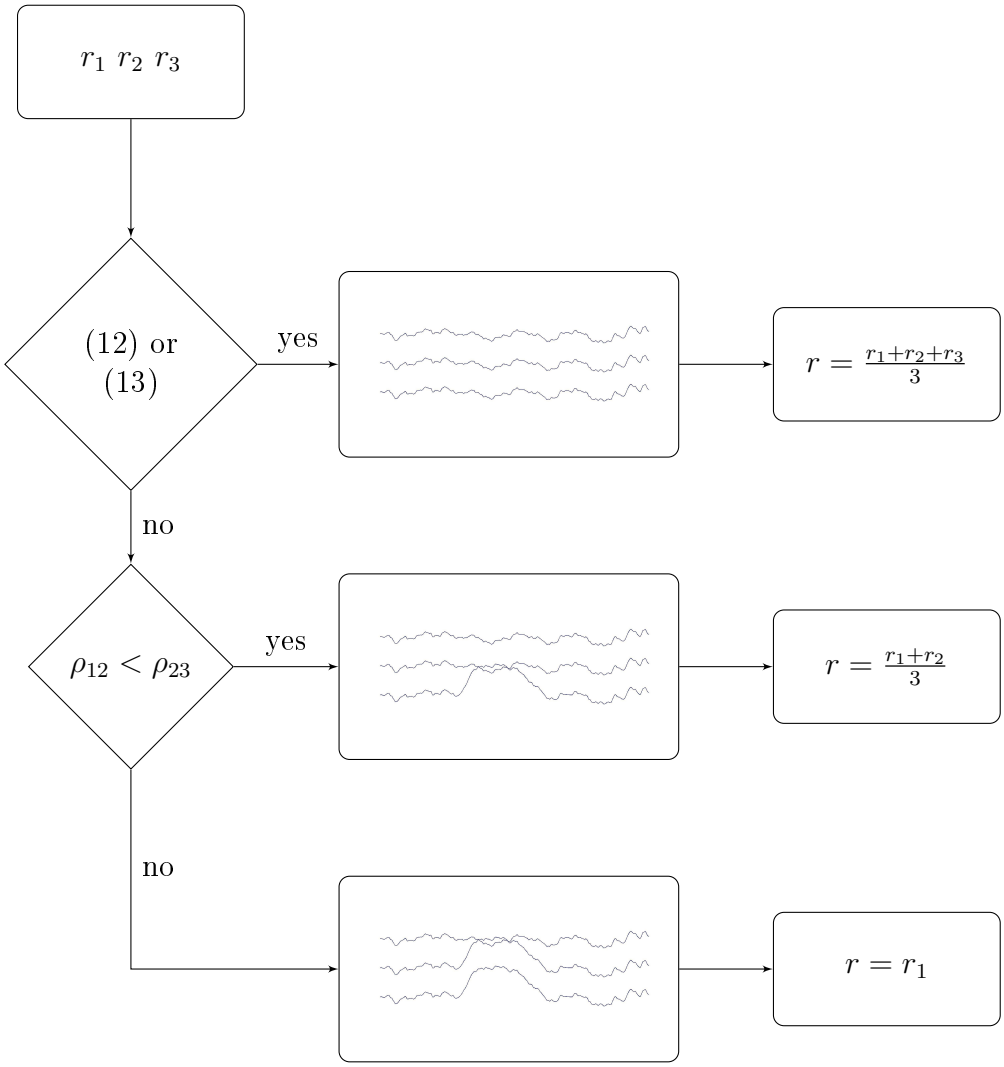

Figure 11: Scheme of combination of partial reconstructions. The first decision means that there are significant difference between $r_1\ r_2\ r_3$. The second decision divides the cases where r_2 contains or not the artifact (note that the r_1 is assumed to be artifact-free).

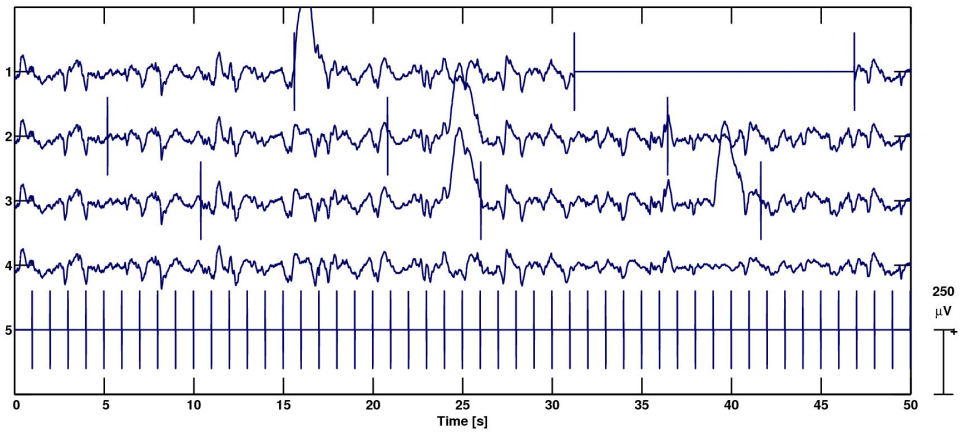

Figure 12: The first three components show simulated partial reconstructions of one channel of the signal, the fourth one shows the final reconstruction. Vertical lines denotes partitioning into frames and segments (shown in the fifth channel).

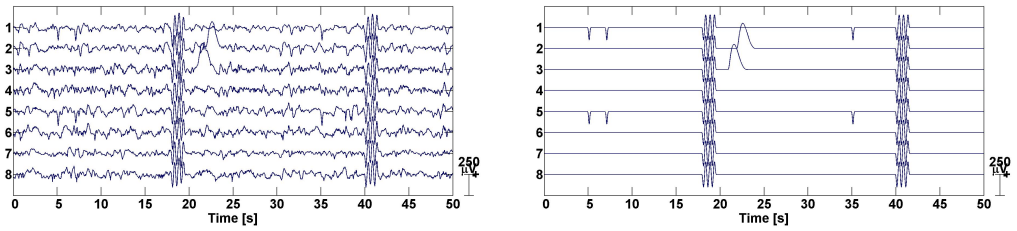

Figure 13: Original signal contaminated by several artificial artifact. The right part of the figure shows the added artifacts.

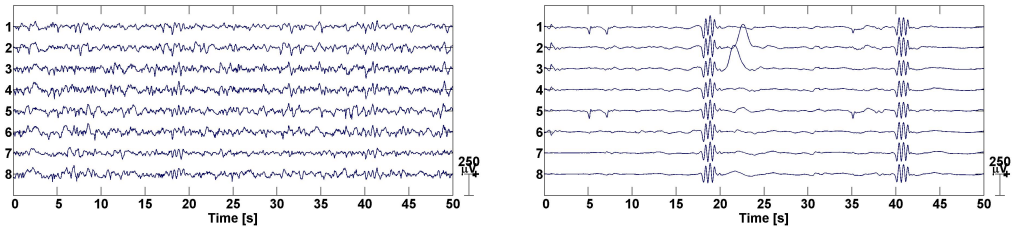

Figure 14: Signal from figure 13 processed by algorithm based on wICA. The right part of the figure shows the estimated artifacts.

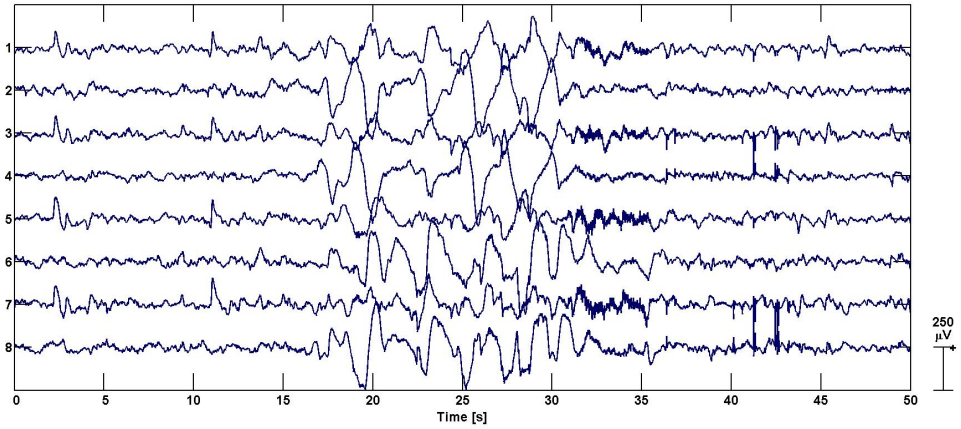

Figure 15: Original data contaminated by real artifacts.

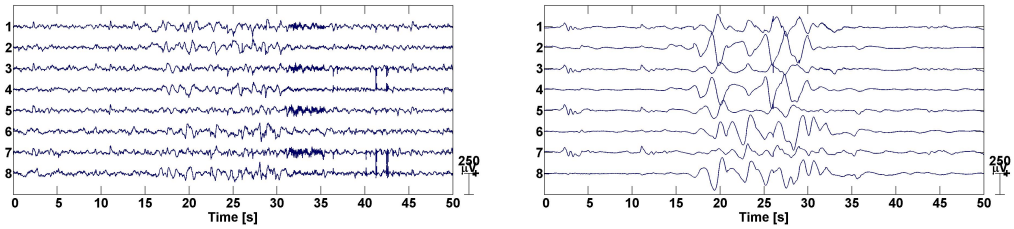

Figure 16: Signal from figure 15 processed by algorithm based on wICA. The right part of the figure shows the estimated artifacts.

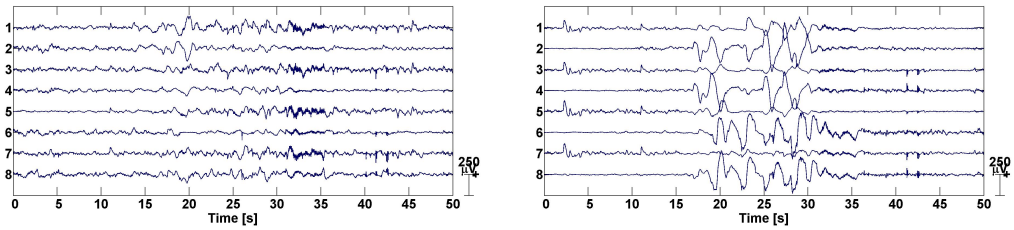

Figure 17: Signal from figure 15 processed by algorithm based on ICA. The right part of the figure shows estimated artifacts.

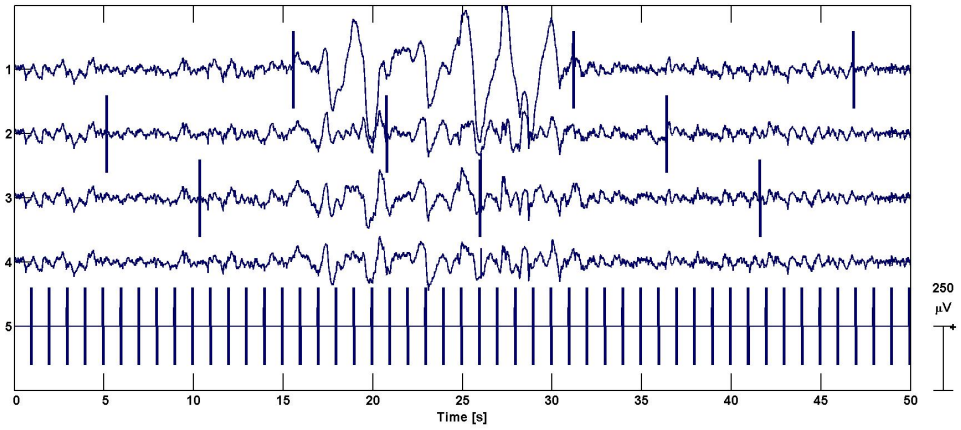

Figure 18: The first three components (channels) show partial reconstructions of the second channel of the signal in figure 15, the fourth channel contains the final reconstruction. Vertical lines denotes partitioning into frames and segments (shown in the fifth channel).

8 Conclusion

The wICA improvement of algorithm for removing artifacts from EEG signal has been presented. The algorithm is suitable for artifacts that have relatively short duration and exceed in magnitude the neighborhood signal and is more robust than the algorithm without wavelet denoising. The method was tested namely on eight-channel neonatal EEG recordings and showed good performance both in artificial and real artifacts removing. Other experiments not included in this report showed that the method can work equally well in scenarios with more channels. In fact, if the number of channels is larger, the artifact removal is easier. Note that the algorithm can be used very efficiently because processing of an eight-channel EEG with 77000 samples ($\approx$10min with 128Hz sampling) takes only about ten second.

Acknowledgements

This work was supported by Ministry of Education, Youth and Sports of the Czech Republic through the project 1M0572 and by Grant Agency of the Czech Republic through the project 102/09/1278.

References

[1] A. Belouchrani, K. Abed-Meraim, J.F. Cardoso, and E. Moulines. A blind source separation technique using second-order statistics. *Signal Processing, IEEE Transactions on*, 45(2):434–444, 2002.

[2] C.S. Burrus, R.A. Gopinath, H. Guo, J.E. Odegard, and I.W. Selesnick. *Introduction to wavelets and wavelet transforms: a primer*. Prentice Hall, Upper Saddle River, NJ, 1998.

[3] N.P. Castellanos and V.A. Makarov. Recovering EEG brain signals: Artifact suppression with wavelet enhanced independent component analysis. *Journal of neuroscience methods*, 158(2):300–312, 2006.

[4] I. Daubechies. *Ten lectures on wavelets*. Society for Industrial Mathematics, 1992.

[5] D.L. Donoho et al. De-noising by soft-thresholding. *IEEE Transactions on Information Theory*, 41(3):613–627, 1995.

[6] A. Hyvärinen and E. Oja. A fast fixed-point algorithm for independent component analysis. *Neural computation*, 9(7):1483–1492, 1997.

[7] C.J. James and C.W. Hesse. Independent component analysis for biomedical signals. *Physiological Measurement*, 26:R15, 2005.

[8] C.A. Joyce, I.F. Gorodnitsky, and M. Kutas. Automatic removal of eye movement and blink artifacts from EEG data using blind component separation. *Psychophysiology*, 41(2):313–325, 2004.

[9] Te-Won Lee. *Independent component analysis theory and applications*. Boston: Kluwer Academic Publishers, 1998.

[10] S. Makeig, A.J. Bell, T.P. Jung, T.J. Sejnowski, et al. Independent component analysis of electroencephalographic data. *Advances in neural information processing systems*, pages 145–151, 1996.

[11] D.T. Pham and J.F. Cardoso. Blind separation of instantaneous mixtures of nonstationary sources. *Signal Processing, IEEE Transactions on*, 49(9):1837–1848, 2002.

[12] S. Romero, M.A. Mañanas, and M.J. Barbanoj. A comparative study of automatic techniques for ocular artifact reduction in spontaneous EEG signals based on clinical target variables: A simulation case. *Computers in biology and medicine*, 38(3):348–360, 2008.

[13] P. Tichavsky and A. Yeredor. Fast approximate joint diagonalization incorporating weight matrices. *Signal Processing, IEEE Transactions on*, 57(3):878–891, 2009.

[14] R. Vigário, J. Sarela, V. Jousmiki, M. Hamalainen, and E. Oja. Independent component approach to the analysis of EEG and MEG recordings. *Biomedical Engineering, IEEE Transactions on*, 47(5):589–593, 2002.

[15] M Zima, P. Tichavský, and V. Krajča. Odstraňování artefaktů v EEG datech III, vyzkumná zpráva ÚTIA AV ČR č. 2259, říjen 2009, 24 pp.

[16] Tichavský, P. and Koldovský, Z. Fast and accurate methods of independent component analysis: A Survey. *Kybernetika* 47(5), 2011, to appear.